

Eliashberg theory of a multiband non-phononic spin glass superconductor

G.A. Ummarino^{1,2}

E-mail: giovanni.ummarino@polito.it

¹ Istituto di Ingegneria e Fisica dei Materiali, Dipartimento di Scienza Applicata e Tecnologia, Politecnico di Torino, Corso Duca degli Abruzzi 24, 10129 Torino, Italy

²National Research Nuclear University MEPhI (Moscow Engineering Physics Institute), Kashirskoe shosse 31, Moscow 115409, Russia

Abstract. I solved the Eliashberg equations for multiband non-phononic $s\pm$ wave spin-glass superconductor and I calculated the temperature dependence of gaps and superfluid density, revealing unusual behaviors such as non monotonic temperature dependence and reentrant superconductivity. The phase diagram, for particular values of input parameters that could describe the iron pnictide $EuFe_2(As_{1-x}P_x)_2$, is still more complex with two different ranges of temperature where the superconductivity appears.

1. Introduction

The discovery of the new iron-based superconductors family based on $EuFe_2As_2$ [1, 2, 3, 4, 5, 6, 7, 8] allowed to investigate more deeply the interplay of magnetism and superconductivity. Compared to the past there is now a new aspect to be considered: not only magnetism competes with superconductivity, but it can also be involved in the mechanism of superconductivity itself, as in the case of cuprates, heavy fermions and iron-based superconductors.

The case of the family of iron-based superconductors $EuFe_2As_2$ [1, 2, 3, 4, 5, 6, 7, 8] is particularly interesting because the ferromagnetic and superconducting transition temperatures are near, where the first is connected to the Eu^{2+} local magnetic moments. It can also happen that the superconducting critical temperature is higher than that of the magnetic ordering [1, 2, 3, 4, 5, 6, 7, 8]. In these systems a complex phenomenology of magnetic phases is observed: below the critical superconducting temperature two distinct magnetic transitions take place, the ordering at higher temperature is associated with the antiferromagnetic interlayer coupling, whereas the behaviour at lower temperature might be identified as the change over to a spin-glass state, where the moments between the layers are decoupled [2, 7]. Usually the spin-glass state [9] occurs in substitutionally disordered alloys [10, 11, 12], where, by means of the long-range Rudermann-Kittel-Kasuya-Yosida interaction, mediated by conduction electrons, the localized magnetic moments, randomly distributed, interact. Because not all magnetic moments can be simultaneously satisfied in their spin orientation with respect to the others, it happens that frustration in the magnetic ordering arises. This fact produces an infinite number of random configurations degenerate in energy but separated by large energy barriers. In this way the ground state cannot evolve into another on the experimental time scale. A typical freezing temperature T_{SG} is associated with the spin-glass state below which the spins freeze into one of these random configurations. The magnetic susceptibility in the spin-glasses shows a cusp at T_{SG} , while nothing happens to specific heat other than a broad maximum around T_{SG} , and no Bragg peaks, which usually are a signal of long-range magnetic order, is found in neutron scattering experiments. The correct order parameter for these systems has to be related to the probability that a spin with a given direction at a finite time will have the same direction in the infinite-time limit. The frozen nature of the spin-glass state is reflected in this order parameter, but no spatial correlations are present as instead happens in other magnetic order parameters. Is it possible to reproduce this phenomenology connected with the superconducting state inside a theory? In this paper I will discuss the predictions of the theory on some physical quantities for a multiband spin-glass non phononic s_{\pm} -wave superconductor in the framework of Eliashberg equations and I will take as example the particular case of $EuFe_2(As_{1-x}P_x)_2$ [5]. Of course I do not claim to reproduce the complex experimental phenomenology of this material but simply to have indications on the input parameters to be included in the Eliashberg equations in the hope that one day it will be possible to find a material where only the

superconducting state and the spin-glass state appear without any other complications. The starting point will be the theoretical work of M.J. Nass [13, 14, 15] and J.P Carbotte [16, 17, 18, 19] that describe a single band spin-glass s-wave phononic superconductor always in the framework of Eliashberg theory.

2. The Model

By introducing the order parameter for the spin-glass state as $q = \lim_{t \rightarrow +\infty} \langle \mathbf{S}_i(t) \cdot \mathbf{S}_i(0) \rangle$ it is possible to describe mathematically this spin freezing [9]. This order parameter is proportional to the probability that a given spin that has a particular direction at $t = 0$ will still orientated in that direction an infinite time later. This situation is quite different from having a order parameter in a ferromagnetic or antiferromagnetic system which reflect space as well as time correlations. Although each spin is essentially fixed in direction, in the absence of a magnetic field, upon averaging over all spins the total spin is zero at all temperatures. By introducing a probability distribution it is possible to reproduce the randomness of the exchange interaction, and then average over this distribution. It is necessary to use the replica approach in order to carry out the averaging of the free energy over this distribution of exchange interactions and succeeded in finding a new order parameter defined as the configuration average of the equal time spin operators at a given site in different replicas of the system [9].

In the past papers [13, 14, 15, 16, 17, 18, 19], the developed theory is on phononic superconductors where it was also added a contribution of antiferromagnetic spin fluctuations (dynamic part) and spin-glass (static part). In this case, it is not necessary to introduce the dynamic part which is already being responsible for the mechanism of superconductivity but only the static part which is formally equal to the contribution of magnetic impurities with an additional dependence on temperature. The antiferromagnetic spin fluctuations have two components [13, 14, 15, 16, 17, 18, 19]: a dynamical component responsible of $s \pm$ superconductivity and a static component responsible to spin-glass behaviour that goes to zero at the spin-glass critical temperature T_{SG} . For $T > T_{SG}$ the static component disappears and the material behaves like a normal $s \pm$ superconductor. In the old phononic low temperature superconductors the dynamic part is, usually, negligible and pair breaking while, in the multiband iron pnictides superconductors, it is the responsible of superconductivity. The contribution of the spin-glass phase can be represented, in an approximate way, in Eliashberg equations, by a term ($\Gamma^M(T)$) similar to that associated with the presence of magnetic impurities but with a temperature dependence. Precisely the magnetic impurities scattering rate [16, 17, 18, 19] that mimics the spin-glass state is $\Gamma^M(T) = \pi N(0) J^2 S^2 [1 - (\frac{T}{T_{SG}})^\beta]$ where $N(0)$ is the total density of states at the Fermi level, J is a exchange constant, S is the spin of the magnetic element and β is a number [16, 17, 18, 19] that can be 1 or 2 depending from the physical characteristic of magnetic element (Eu in this case) and of the host material (the specific iron pnictides). At this moment there are not enough data to understand if

β is 1 or 2 so I solve the Eliashberg equations in the two cases. This theory stems from the desire to build a very simple model that still manages to grasp the fundamental physics of a multiband spin-glass superconductor. More sophisticated theories [20] start from multi-orbital Hubbard models that produce richer phase diagrams and also triplet superconductivity. For solving the Eliashberg equations are necessary a lot of input parameters connected with the characteristic of physical system. In the following I will refer to $EuFe_2(As_{0.835}P_{0.165})_2$ a material [5] of iron pnictides family. The electronic structure of the compound $EuFe_2(As_{0.835}P_{0.165})_2$ can be approximately described, in principle, as almost all electrons doped iron-based materials, by a three-band model with two electron bands (indicated in the following as bands 1 and 2) and one hole band (indicated in the following as band 3) [21]. In this way the gap of hole band, Δ_3 , has opposite sign to the gaps residing on the electrons bands Δ_1 and Δ_2 . This compound is especially fascinating since, despite the proximity of the magnetic and superconducting phases observed at rather high temperatures, there is just a little variation of their transition temperatures to these two phases [5]. The same happens for the stoichiometric material $RbEuFe_4As_4$ where the superconductivity and a long range magnetic orders exist independently from each other [22]. In this simple model the effect of spin-glasses are simulated by some functions of temperature $\Gamma_{jk}^M(T)$ that go to zero before T_c (precisely to $T_{SG} < T_c$) and in this way they do not affect the critical temperature but change the behaviour of some physical quantities below T_c .

In the iron pnictides the phonons are responsible for the intraband coupling (*ph*) [24] and usually are neglected while the antiferromagnetic spin fluctuations (*sf*) are connected to interband coupling between holes and electrons bands ($s\pm$ wave model [23, 24]). With the intention to reduce the number of free parameters I use an effective two-band model (band 1 electrons, band 2 holes) where it is not possible to set to zero the intraband coupling and where the electron-boson coupling constants have not an immediate interpretation [27, 28] because this model simulates the true physical situation (three bands) with effective values of electron boson coupling constants in a two bands model. I investigate what happens in a multiband system and, for simplicity, I study a two bands system that simulates a real three bands system. In the following the $s\pm$ wave two bands Eliashberg equations [25, 26, 29] are written. To calculate the critical temperature and the gaps, it is necessary to solve 4 coupled equations: 2 for the renormalization functions $Z_j(i\omega_n)$ and 2 for the gaps $\Delta_j(i\omega_n)$, where j, k are band index (that range between 1 and 2) and ω_n are the Matsubara frequencies. The imaginary-axis equations [30, 31, 32] read:

$$\begin{aligned} \omega_n Z_j(i\omega_n) &= \omega_n + \pi T \sum_{m,k} \Lambda_{jk}^Z(i\omega_n, i\omega_m) N_k^Z(i\omega_m) + \\ &+ \sum_k [\Gamma_{jk}^N + \Gamma_{jk}^M(T)] N_k^Z(i\omega_n) \end{aligned} \quad (1)$$

$$Z_j(i\omega_n) \Delta_j(i\omega_n) = \pi T \sum_{m,k} [\Lambda_{jk}^\Delta(i\omega_n, i\omega_m) - \mu_{jk}^*(\omega_c)] \times$$

$$\times \Theta(\omega_c - |\omega_m|) N_k^\Delta(i\omega_m) + \sum_k [\Gamma_{jk}^N - \Gamma_{jk}^M(T)] N_k^\Delta(i\omega_n) \quad (2)$$

where Γ_{jk}^N and $\Gamma_{jk}^M(T)$ are the scattering rates from non-magnetic and magnetic impurities that, in this model, represent the term connected with the spin-glass phase. For spin-glass superconductors the magnetic impurities scattering rates are $\Gamma_{jk}^M(T) = c_{jk}\pi N(0)J^2S^2[1 - (\frac{T}{T_{SG}})^\beta] = k_{jk}[1 - (\frac{T}{T_{SG}})^\beta]$ where c_{jk} are weight connected with the bands ($\frac{c_{jk}}{c_{kj}} = \frac{N_k(0)}{N_j(0)}$ as the usual impurity scattering rates [30, 31, 32]) and, of course, $k_{jk} = c_{jk}\pi N(0)J^2S^2$. I put the non magnetic scattering rates Γ_{jk}^N equal to zero because I suppose to have good single crystals (no disorder). In the previous equations I have $\Lambda_{jk}^Z(i\omega_n, i\omega_m) = \Lambda_{jk}^{ph}(i\omega_n, i\omega_m) + \Lambda_{jk}^{sf}(i\omega_n, i\omega_m)$ and $\Lambda_{jk}^\Delta(i\omega_n, i\omega_m) = \Lambda_{jk}^{ph}(i\omega_n, i\omega_m) - \Lambda_{jk}^{sf}(i\omega_n, i\omega_m)$ where

$$\Lambda_{jk}^{ph,sf}(i\omega_n, i\omega_m) = 2 \int_0^{+\infty} d\Omega \Omega \alpha_{jk}^2 F_{jk}^{ph,sf}(\Omega) / [(\omega_n - \omega_m)^2 + \Omega^2],$$

Θ is the Heaviside function and ω_c is a cutoff energy. The quantities $\mu_{jk}^*(\omega_c)$ are the elements of the 2×2 Coulomb pseudopotential matrix and finally, $N_k^\Delta(i\omega_m) = \Delta_k(i\omega_m) / \sqrt{\omega_m^2 + \Delta_k^2(i\omega_m)}$ and $N_k^Z(i\omega_m) = \omega_m / \sqrt{\omega_m^2 + \Delta_k^2(i\omega_m)}$. The electron-boson coupling constants are defined as $\lambda_{jk}^{ph,sf} = 2 \int_0^{+\infty} d\Omega \frac{\alpha_{jk}^2 F_{jk}^{ph,sf}(\Omega)}{\Omega}$.

In order to have the smallest number of free parameter and the simplest model that still grasps the physics of this system, I make further assumptions that have been shown to be valid for iron pnictides [32, 30, 31]. I assume, following ref. [24] that the total electron-phonon coupling constant is small (the upper limit of the phonon coupling in the usual iron-arsenide compounds is ≈ 0.35 [33]) so I put, in first approximation, the phonon contribution equal to zero ($\lambda_{jk}^{ph} = 0$) and as, following Mazin [34], the Coulomb pseudopotential matrix: $\mu_{jj}^*(\omega_c) = \mu_{jk}^*(\omega_c) = 0$ [32, 30, 31, 34]. After all these approximations, I write the electron-boson coupling constant matrix λ_{jk} in this way: [32, 30, 31, 35]:

$$\lambda_{jk} = \begin{pmatrix} \lambda_{11}^{sf} & \lambda_{12}^{sf} \\ \lambda_{21}^{sf} = \lambda_{12}^{sf} \nu_{12} & \lambda_{22}^{sf} \end{pmatrix} \quad (3)$$

where $\nu_{12} = N_1(0)/N_2(0)$, and $N_j(0)$ is the normal density of states at the Fermi level for the j -th band. Based on experimental data and theoretical calculations [32, 30, 31] I choose for the electron-antiferromagnetic spin fluctuation spectral functions $\alpha_{jk}^2 F_{jk}^{sf}(\Omega)$ a Lorentzian shape, i.e.:

$$\alpha_{jk}^2 F_{jk}^{sf}(\Omega) = C_{jk} \left\{ \frac{1}{(\Omega + \Omega_{jk})^2 + Y_{jk}^2} - \frac{1}{(\Omega - \Omega_{jk})^2 + Y_{jk}^2} \right\}, \quad (4)$$

where C_{jk} are normalization constants, necessary to obtain the proper values of λ_{jk}^{sf} , while Ω_{jk} and Y_{jk} are the peak energies and the half-widths of the Lorentzian functions, respectively [32]. Following the experimental data [36] I put $\Omega_{jk} = \Omega_0$, i.e. I assume that the characteristic energy of spin fluctuations is a single quantity for all the coupling channels, and $Y_{jk} = \Omega_0/2$. The spectral function used here, normalized to one, is shown in the inset (a) of Fig 1.

The factors ν_{jk} that enter in the definition of λ_{jk} (eq. 3) are unknown so I assume that they are equal, for example, to the $Ba(Fe_{1-x}Rh_x)_2As_2$ electron doped case [37] so $\nu_{12} = 0.8333$ as well as the coupling constants [37] and I change lightly just the value of λ_{22} for obtaining the correct critical temperature $T_c = 22$ K. At the end the values are $\lambda_{11} = 1.00$, $\lambda_{12} = -0.17$ and $\lambda_{22} = 2.65$ for a averaged coupling constant $\lambda_t = \frac{\sum_{jk} N_j(0) \lambda_{jk}}{\sum_j N_j(0)} = 1.75$. For iron pnictides it was experimentally found [38, 39] that the empirical law $\Omega_0 = 2T_c/5$ holds, therefore the value of the energy peak Ω_0 of the Eliashberg spectral functions $\alpha_{jk}^2 F_{jk}^{sf}(\Omega)$ is fixed. To finish, in the numerical calculations I used a cut-off energy $\omega_c = 180$ meV. These input parameters produce, by numerically solving the Eliashberg equations, exactly a critical temperature of 22 K.

3. Calculation of superconducting gaps

In the iron pnictides, usually, the impurities are almost all concentrated in one band: i.e. in the hole band for the electron doped materials as this case and in the electron band [40, 41] for the hole doped materials [42]. This means that, in the electrons doped materials, $k_{22} \gg k_{11}, k_{12}$. I choose $k_{11} = k_{12} = 0.2k_{22}$ as happen in the $Ba(Fe_{1-x}Co_x)_2As_2$ [40]. By using the typical parameters of iron pnictides and spin-glass systems I find that $k_{22} \simeq 3.1$ meV ($N(0) = 5.6$ states/eV, $S = 7/2$, $J = 0.12$ meV and $T_{SG} = 15$ K) [5, 43]. Because the true values of the parameters in the last bracket are just approximative I solve the Eliashberg equations for values close to 3.1 as $k_{22} = 0, 1, 2, 3, 3.5, 4, 4.05, 5$ meV in the two cases: $\beta = 1$ and $\beta = 2$. In the ideal case it would be necessary to know the law that links T_{SG} at the value of k_{22} . Here $T_{SG} = 15$ K is an experimental input [5]. In the Figs 1 and 2 the temperature dependence of gaps $\Delta_{1,2}(i\omega_{n=0})$ are shown. It is possible to see in Fig 1 that the absolute values of the gaps with increasing temperature at first increases until T_{SG} , and then decreases. This behaviour appears when magnetic impurities (also without temperature dependence) and disorder are present, both in $s++$ and $s\pm$ superconductor or if only disorder is present in $s\pm$ two bands superconductor [44].

For $k_{22} = 5$ meV and $\beta = 1$, reentrant superconductivity is obtained. As it is shown in Fig 2 in the case $\beta = 1$ the effect is similar but stronger and, besides having reentrant superconductivity for $k_{22} = 5$ meV, it is possible to see an even more complex situation for $k_{22} = 4.05$ meV. In the last case the system has three different critical temperatures: I think that it would be difficult to observe this behaviour in a real system because it arises from a fine tuning of the input parameter. In a s-wave superconductor the magnetic order destroys the superconductivity but the temperature weakens both the magnetic order and the coupling between the electrons in the Cooper pairs so the "reentrant" behaviour can emerge from the balance between the effect of magnetism and temperature. I solved the Eliashberg equations, for completeness, also in the case $k_{12} = 0.2k_{22}$ and $k_{11} = k_{22}$ always with $\beta = 1$ and $\beta = 2$. The results are shown in Fig 3 and are similar to previous ones in the general trend as a function of the value of k_{22} . In all case, of course, for $T > T_{SG}$ the effect of "magnetic impurities" disappeared and the behaviour is the same of a standard two bands superconductor.

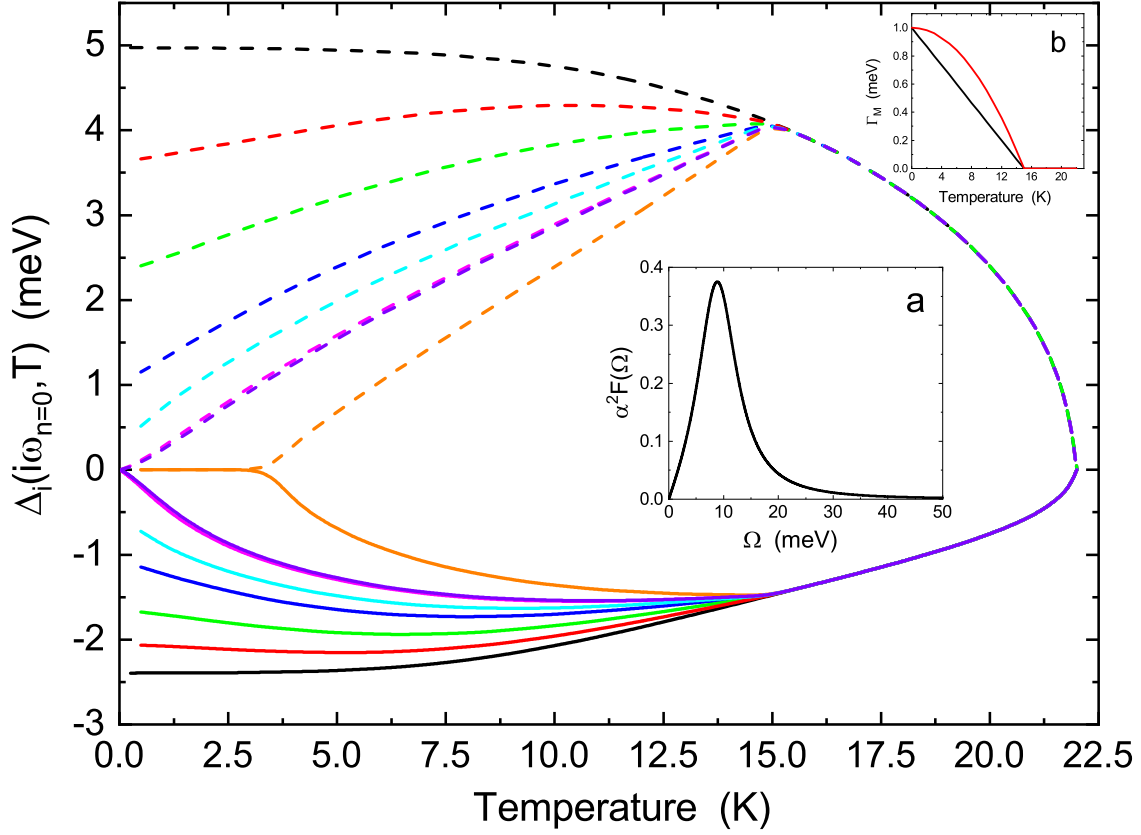


Figure 1. (Color online) The gaps $\Delta_i(i\omega_{n=0})$ in function of temperature obtained by solving the Eliashberg equations on imaginary axis: solid lines for $\Delta_1(i\omega_{n=0})$, dashed lines for $\Delta_2(i\omega_{n=0})$ in the case $k_{11} = k_{12} = 0.2k_{22}$ and $\beta = 1$. Black lines for $k_{22} = 0$ meV, red lines for $k_{22} = 1$ meV, green lines for $k_{22} = 2$ meV, dark blue lines for $k_{22} = 3$ meV, cyan line for $k_{22} = 3.5$ meV, magenta lines for $k_{22} = 4$ meV, violet lines for $k_{22} = 4.05$ meV and orange lines for $k_{22} = 5$ meV. In the inset (a) the antiferromagnetic spin fluctuations function, normalized to one, is shown while in the inset (b) the temperature dependence of k_{jk} is shown (black solid line $\beta = 1$ and red solid line $\beta = 2$) with $k_{jk} = 1$.

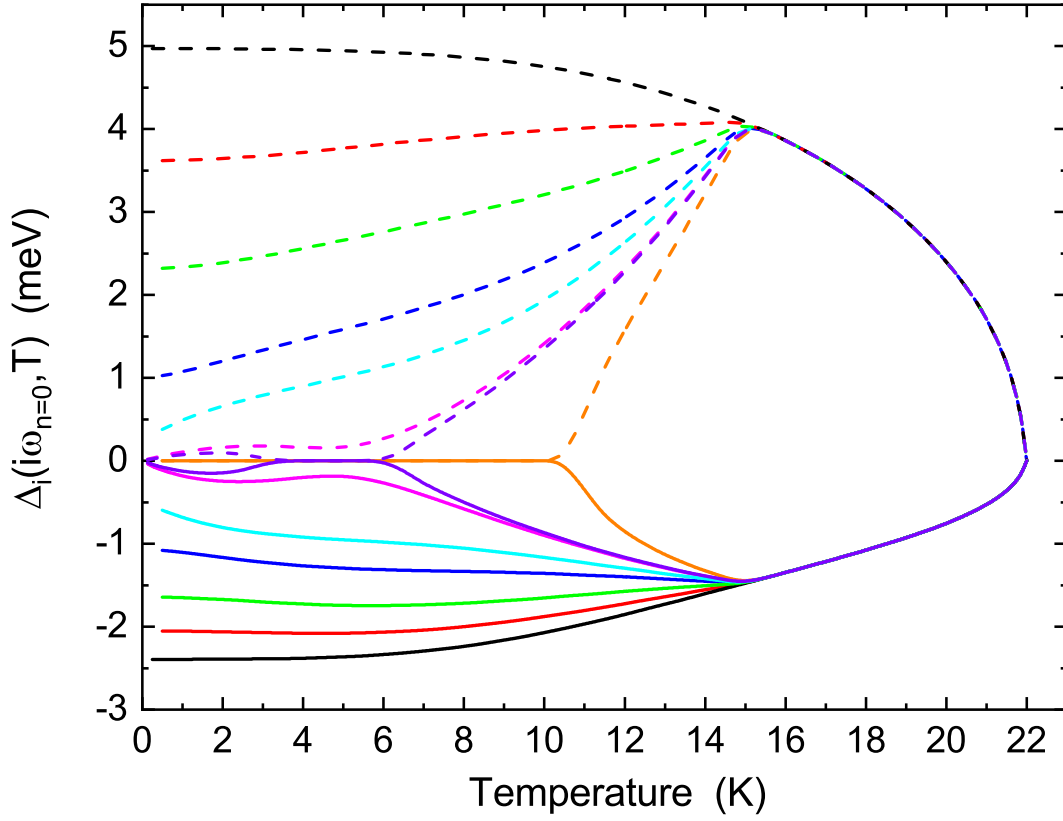


Figure 2. (Color online) The gaps $\Delta_i(i\omega_{n=0})$ in function of temperature obtained by solving the Eliashberg equations on imaginary axis: solid lines for $\Delta_1(i\omega_{n=0})$, dashed lines for $\Delta_2(i\omega_{n=0})$ in the case $k_{11} = k_{12} = 0.2k_{22}$ and $\beta = 2$. Black lines for $k_{22} = 0$ meV, red lines for $k_{22} = 1$ meV, green lines for $k_{22} = 2$ meV, dark blue lines for $k_{22} = 3$ meV, cyan line for $k_{22} = 3.5$ meV, magenta lines for $k_{22} = 4$ meV, violet lines for $k_{22} = 4.05$ meV and orange lines for $k_{22} = 5$ meV.

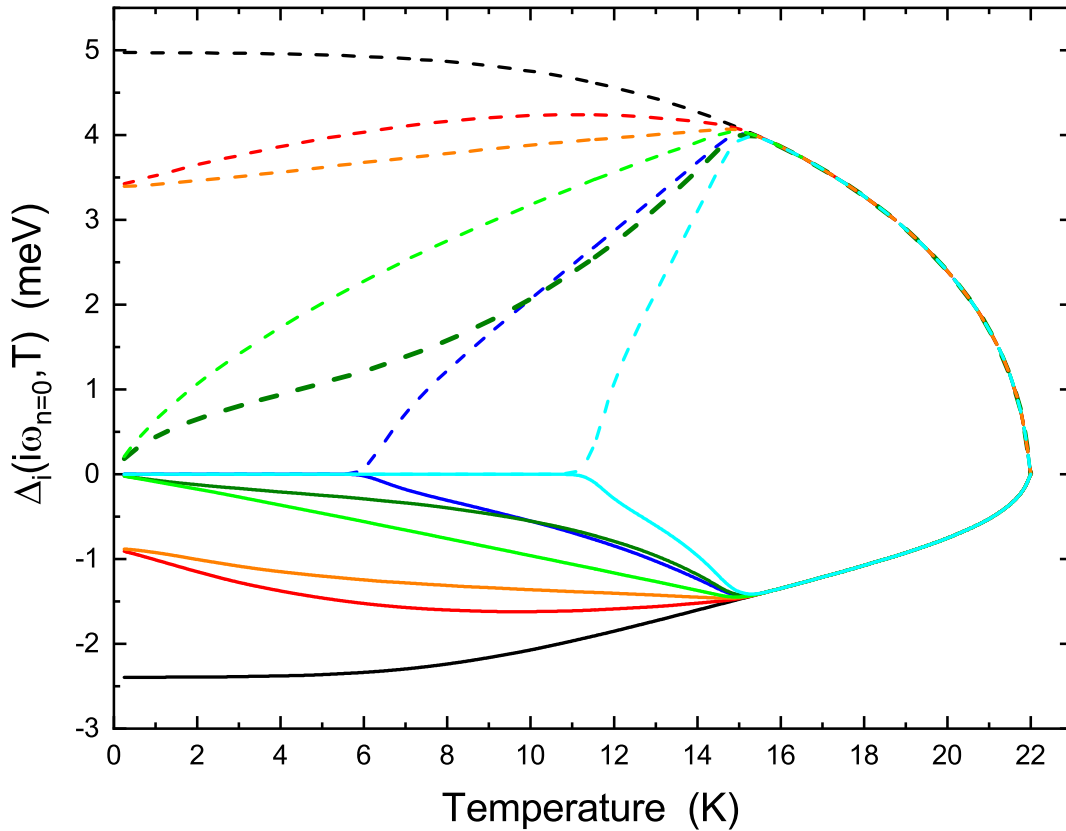


Figure 3. (Color online) The gaps $\Delta_i(i\omega_{n=0})$ in function of temperature obtained by solving the Eliashberg equations on imaginary axis: solid lines for $\Delta_1(i\omega_{n=0})$, dashed lines for $\Delta_2(i\omega_{n=0})$ in the case $k_{11} = k_{22} = 5k_{12}$. Black lines for $k_{22} = 0$ meV, red lines for $k_{22} = 1$ meV and $\beta = 1$, orange lines for $k_{22} = 1$ meV and $\beta = 2$, green lines for $k_{22} = 3$ meV and $\beta = 1$, olive lines for $k_{22} = 3$ meV and $\beta = 2$, dark blue lines for $k_{22} = 5$ meV and $\beta = 1$ and magenta lines for $k_{22} = 5$ meV and $\beta = 2$.

4. Calculation of the penetration depth

The penetration depth (or the superfluid density as it is shown in Figs. 4, 5 and 6) can be computed starting from the renormalization functions $Z_j(i\omega_n)$ and the gaps $\Delta_j(i\omega_n)$ by using the following formula: [45]

$$\lambda^{-2}(T) = \left(\frac{\omega_p}{c}\right)^2 \sum_{j=1}^2 w_j \pi T \sum_{n=-\infty}^{+\infty} \frac{\Delta_j^2(\omega_n) Z_j^2(\omega_n)}{[\omega_n^2 Z_j^2(\omega_n) + \Delta_j^2(\omega_n) Z_j^2(\omega_n)]^{3/2}} \quad (5)$$

where $\omega_{p,i}$ is the plasma frequency of the i -th band and ω_p is the total plasma frequency in order that the $w_j = (\omega_{p,j}/\omega_p)^2$ are the weights of the single bands.

The low-temperature value of the penetration depth $\lambda_L(0)$ should, in principle, be related to the plasma frequency by $\omega_p = c/\lambda_L(0)$ [46] and appears as a multiplicative factor of the summation. Here $w_1 = 0.72$ and $w_2 = 0.28$ as in the Co doped iron compounds [40]. In principle, it is important the calculation of superfluid density

(penetration depth) in order to compare theoretical predictions with experiment because it is easier to find these measurements in literature [47]. In the Figs 4, 5 the superfluid density in function of temperature is shown when $k_{11} = k_{12} = 0.2k_{22}$, $k_{22} = 0, 1, 2, 3, 3.5, 4, 4.05, 5$ meV with $\beta = 1$ and $\beta = 2$. In Fig. 6 I show the superfluid density when $k_{12} = 0.2k_{11} = 0.2k_{22}$, $k_{22} = 0, 1, 3, 5$ meV with $\beta = 1$ and $\beta = 2$. These results are a clear prediction of possible situations that can be easily identified. Unfortunately, there is still no experimental data to compare with these theoretical predictions. The behavior of the penetration depth as a function of temperature shows how the presence of a spin-glass state in competition with superconductivity substantially changes the phase diagram of a superconductor making it extremely richer. Also for the superfluid density it is clear when reentrant superconductivity appears as well as the case of three critical temperatures (see Fig 5 violet line). In the Figs 1 and 2 in the cases with $k_{22} = 4.00$ meV and $k_{22} = 4.05$ meV the values of $\Delta_1(i\omega_{n=0})$ and $\Delta_2(i\omega_{n=0})$, at very low temperatures, are almost zero but the corresponding superfluid density at the same temperatures is different from zero in an appreciable way. As is it possible? From the numerical solution of Eliashberg equation in the standard case (when the k_{jk} are equal to zero) the maximum value of $|\Delta_i(i\omega_n)|$ is for $n = 0$ and the $|\Delta_i(i\omega_n)|$ decreases when $|n|$ increases while, when the k_{jk} are different from zero, the dependence from $|n|$ is different and not usual. In the inset of Fig. 5 the calculated values of $\Delta_1(i\omega_n)$ and $\Delta_2(i\omega_n)$, in the $k_{22} = 4.05$ meV and $\beta = 2$ case at $T = 0.125$ K, in function of n is shown. In this case it is possible to see that the dependence of $\Delta_j(i\omega_n)$ from n is not standard. In this case the maximum value of $|\Delta_i(i\omega_n)|$ is not more for $n = 0$ so also if $\Delta_i(i\omega_{n=0}) \simeq 0$ meV the corresponding superfluid density can be different from zero.

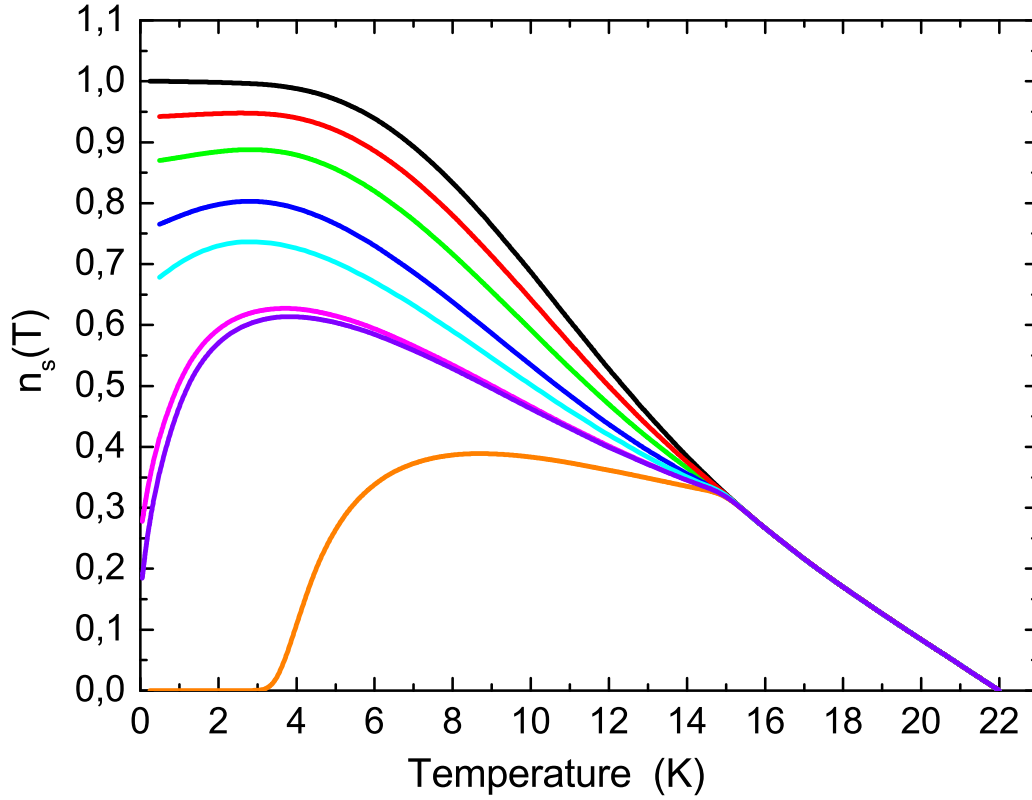


Figure 4. (Color online) The superfluid density $n_s(T)$, normalized at the value at $T=0$ K in the case $k_{22} = 0$, in function of temperature, obtained by solving the Eliashberg equations on imaginary axis in the case $k_{11} = k_{12} = 0.2k_{22}$ and $\beta = 1$. Black line for $k_{22} = 0$ meV, red line for $k_{22} = 1$ meV, green line for $k_{22} = 2$ meV, dark blue line for $k_{22} = 3$ meV, cyan line for $k_{22} = 3.5$ meV, magenta lines for $k_{22} = 4$ meV, violet lines for $k_{22} = 4.05$ meV and orange line for $k_{22} = 5$ meV.

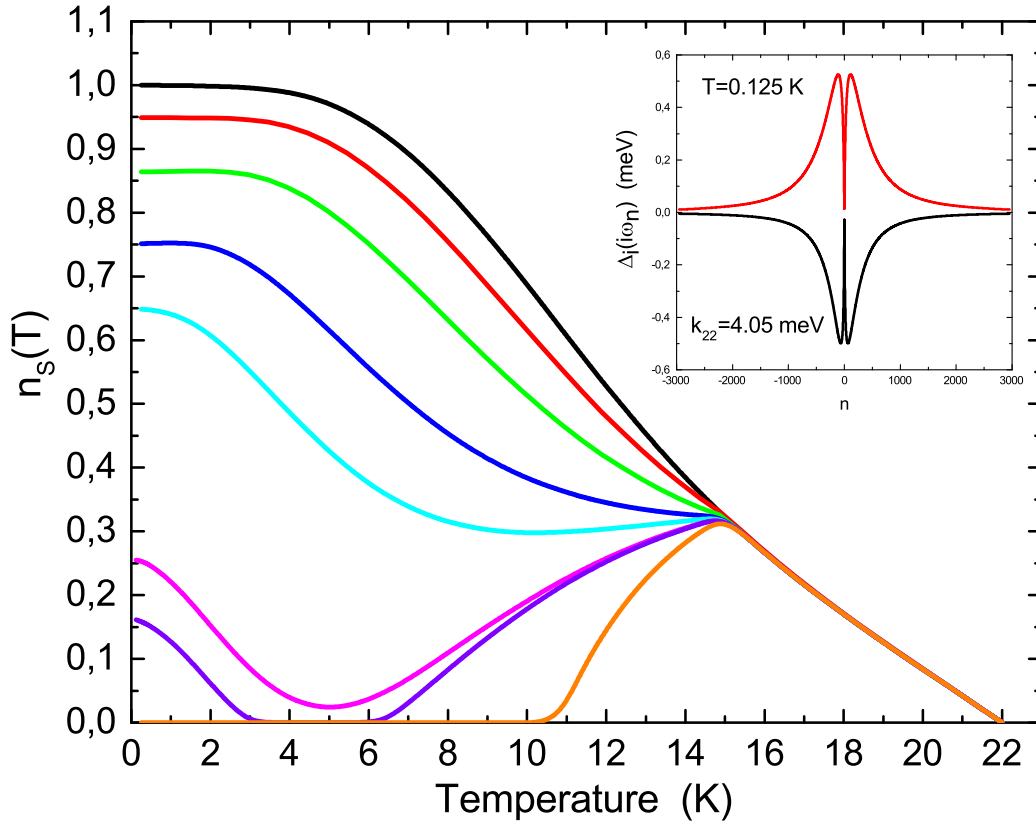


Figure 5. (Color online) The superfluid density $n_s(T)$, normalized at the value at $T=0$ K in the case $k_{22} = 0$, in function of temperature, obtained by solving the Eliashberg equations on imaginary axis in the case $k_{11} = k_{12} = 0.2k_{22}$ and $\beta = 2$. Black line for $k_{22} = 0$ meV, red line for $k_{22} = 1$ meV, green line for $k_{22} = 2$ meV, dark blue line for $k_{22} = 3$ meV, cyan line for $k_{22} = 3.5$ meV, magenta line for $k_{22} = 4$ meV, violet lines for $k_{22} = 4.05$ meV and orange line for $k_{22} = 5$ meV. In the inset, the dependence, obtained by numerical solution of Eliashberg equations in the $k_{22} = 4.05$ meV case at $T = 0.125$ K, of the two order parameters $\Delta_j(i\omega_n)$ from the index n is shown.

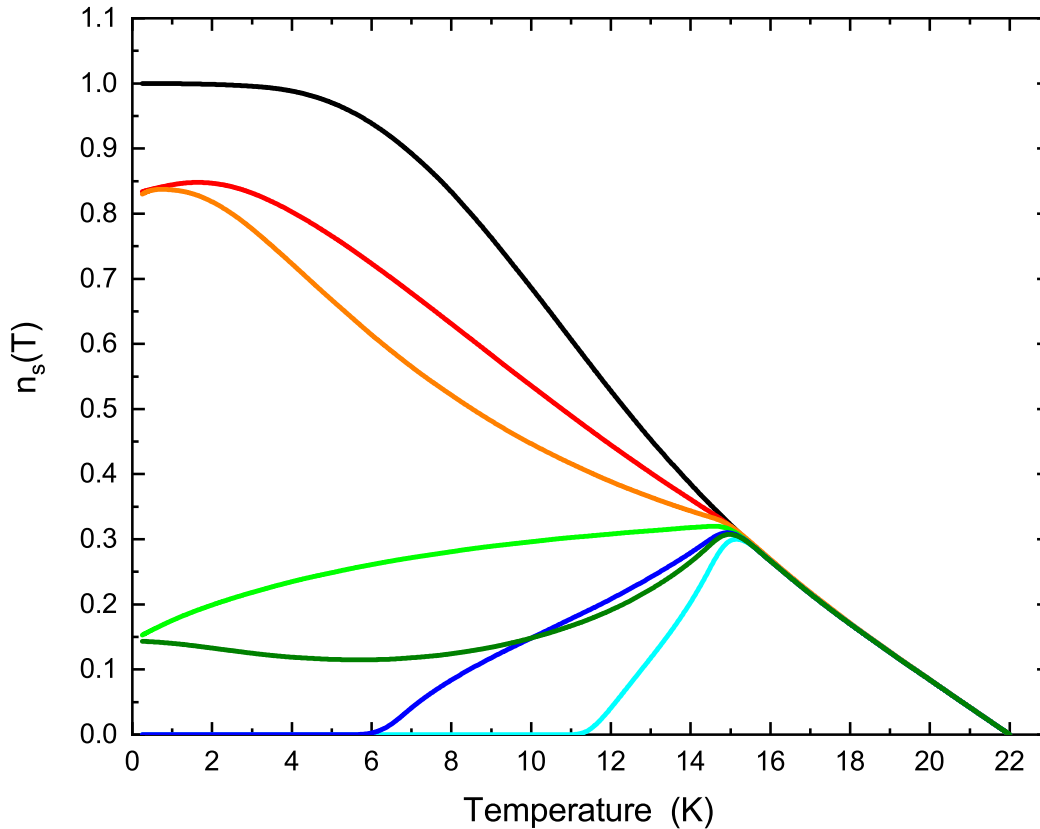


Figure 6. (Color online) The superfluid density $n_s(T)$, normalized at the value at $T=0$ K in the case $k_{22} = 0$, in function of temperature obtained by solving the Eliashberg equations on imaginary axis in the case $k_{11} = k_{22} = 5k_{12}$. Black line for $k_{22} = 0$ meV, red line for $k_{22} = 1$ meV and $\beta = 1$, orange line for $k_{22} = 1$ meV and $\beta = 2$, green line for $k_{22} = 3$ meV and $\beta = 1$, olive line for $k_{22} = 3$ meV and $\beta = 2$, dark blue line for $k_{22} = 5$ meV and $\beta = 1$ and magenta line for $k_{22} = 5$ meV and $\beta = 2$.

5. Conclusions

In conclusion, I have calculated the temperature dependence of gaps and superfluid densities for a two bands non phononic $s\pm$ -wave spin-glass superconductor. In general, the temperature dependence of superconducting properties shows a lot of different behaviours that should be observable in experiment. In this system two competing orders modulated by temperature are present. The magnetic order breaks down the superconductivity, but in this case it also dependent on temperature as well as the superconducting electron-boson coupling. The temperature weakens both but in a different manner so from this competition can born a more complex phase diagram. In addition, reentrant behavior could be a possible signature of a spin-glass state.

6. ACKNOWLEDGMENTS

The author acknowledges support from the MEPhI Academic Excellence Project (Contract No. 02.a03.21.0005).

- [1] S. Nandi, W.T. Jin, Y. Xiao, Y. Su, S. Price, D.K. Shukla, J. Stremper, H.S. Jeevan, P. Gegenwart, and Th. Bruckell, *Phys.Rev. B* **89**, 014512 (2014).
- [2] G. Ghigo, D. Torsello, L. Gozzelino, T. Tamegai, I.S. Veshchunov, S. Pyon, W. Jiao, G.-H. Cao, S. Yu. Grebenchuk, I.A. Golovchanskiy, V.S. Stolyarov, and D. Roditchev, *Physical Review Research* **1**, 033110 (2019).
- [3] W.T. Jin, Y. Xiao, Y. Su, S. Nandi, W.H. Jiao, G. Nisbet, S. Demirdis, G.H. Cao, and Th. Bruckell, *Phys.Rev. B* **93**, 024517 (2016).
- [4] Yi Liu, Ya-Bin Liu, Zhang-Tu Tang, Hao Jiang, Zhi-Cheng Wang, Abduweli Ablimit, Wen-He Jiao, Qian Tao, Chun-Mu Feng, Zhu-An Xu, and Guang-Han Cao, *Phys.Rev. B* **93**, 214503 (2016).
- [5] S. Zapf, H.S. Jeevan, T. Ivek, F. Pfister, F. Klingert, S. Jiang, D. Wu, P. Gegenwart, R.K. Kremer, and M. Dressel, *Phys.Rev. Lett.* **110**, 237002 (2013).
- [6] David Neubauer, Artem V. Pronin, Sina Zapf, Johannes Merz, Hirale S. Jeevan, Wen-He Jiao, Philipp Gegenwart, Guang-Han Cao, and Martin Dressel, *Phys. Status Solidi B* **254**, 1600148 (2017).
- [7] Sina Zapf and Martin Dressel, *Rep. Prog. Phys.* **80** 016501 (2017).
- [8] G. Ghigo, D. Torsello, R. Gerbaldo, L. Gozzelino, S. Pyon, I.S. Veshchunov, T. Tamegai and G-H Cao, *SUST* **33**, 094011 (2020).
- [9] M Mezard, G Parisi, M Virasoro, *Spin glass theory and beyond: An Introduction to the Replica Method and Its Applications* World Scientific Publishing Company, (1987).
- [10] D. Davidov, K. Baberschke, J. A. Mydosh, and G.J. Nieuwenhuys, *J. Phys. F* **7**, L47 (1977).
- [11] S.L. Bud'ko, J. D. Strand, N.E. Anderson, Jr., R.A. Ribeiro, and P.C. Canfield, *Phys.Rev. B* **68**, 104417 (2003).
- [12] S.L. Bud'ko, V.G. Kogan, H. Hodovanets, S. Ran, S.A. Moser, M.J. Lampe, and P.C. Canfield, *Phys.Rev. B* **82**, 174513 (2010).
- [13] M.J. Nass, K. Levin and G.S. Grest, *Phys. Rev. Lett.* **45**, 2070 (1980).
- [14] M.J. Nass, K. Levin and G.S. Grest, *Phys. Rev. B* **23**, 1111 (1981).
- [15] M.J. Nass, K. Levin and G.S. Grest, *Phys. Rev. B* **25**, 4541 (1982).
- [16] W. Stephan and J. P. Carbotte, *Journal of Low Temperature Physics*, **83**, 131, (1991).
- [17] E. Schachinger, W. Stephan, and J.P. Carbotte, *Phys. Rev. B* **37**, 5003 (1988).
- [18] E.J. Nicol and J.P. Carbotte, *Phys. Rev. B* **45**, 10509 (1992).
- [19] A. Perez Gonzalez, E.J. Nicol, and J.P. Carbotte, *Phys. Rev. B* **45**, 5055 (1992).
- [20] S. Hoshino and P. Werner, *Phys. Rev. Lett.* **115**, 247001 (2015); K. Steiner, S. Hoshino, Y. Nomura, and P. Werner, *Phys. Rev. B* **94**, 075107 (2016); S. Hoshino and P. Werner, *Phys. Rev. Lett.* **118**, 177002 (2017); P. Werner, S. Hoshino, and H. Shinaoka, *Phys. Rev. B* **94**, 245134 (2016); P. Werner, X. Chen, and E. Gull, arXiv:1912.01260 (2019).
- [21] D. Torsello, G. A. Ummarino, L. Gozzelino, T. Tamegai, and G. Ghigo *Phys. Rev. B* **99**, 134518 (2019).
- [22] T.K. Kim, K.S. Pervakov, D.V. Evtushinsky, S.W. Jung, G. Poelchen, K. Kummer, V.A. Vlasenko, V.M. Pudalov, D. Roditchev, V.S. Stolyarov, D.V. Vyalikh, V. Borisov, R. Valenti, A. Ernst, S.V. Ereemeev, and E.V. Chulkov, arXiv:2008.00736v1.
- [23] P.J. Hirschfeld, M.M. Korshunov and I.I. Mazin, *Rep. Prog. Phys.* **74**, 124508 (2011).
- [24] I.I. Mazin, D.J. Singh, M.D. Johannes, and M.H. Du, *Phys. Rev. Lett.* **101**, 057003 (2008). *Phys.Rev. B* **84**, 174511 (2011)
- [25] G.M. Eliashberg, *Sov. Phys. JETP* **11**, 696 (1960).
- [26] A.V. Chubukov, D. Pines, and J. Schmalian, *A Spin Fluctuation Model for d-Wave Superconductivity*, D. Manske, I. Eremin, and K.H. Bennemann, *Electronic Theory for*

- Superconductivity in high- T_c Cuprates and Sr_2RuO_4* , K.H. Bennemann and J.B. Ketterson Editors, Volume II. Superconductivity: Novel Superconductors, Springer-Verlag Berlin Heidelberg (2008).
- [27] A. Charnukha, O.V. Dolgov, A.A. Golubov, Y. Matiks, D L. Sun, C.T. Lin, B. Keimer, and A.V. Boris, *Phys. Rev. B* **84**, 174511 (2011).
- [28] D. Torsello, K. Cho, K.R. Joshi, S. Ghimire, G.A. Ummarino, N.M. Nusran, M.A. Tanatar, W.R. Meier, M. Xu, S.L. Bud'ko, P.C. Canfield, G. Ghigo, and R. Prozorov, *Phys. Rev. B* **100**, 094513 (2019).
- [29] D. Torsello, G.A. Ummarino, R. Gerbaldo, L. Gozzelino, G. Ghigo, *J Supercond Nov Magn* **33** 23192324 (2020).
- [30] G.A. Ummarino, M. Tortello, D. Daghero, R.S. Gonnelli, *Phys. Rev. B* **80**, 172503 (2009).
- [31] G.A. Ummarino, M. Tortello, D. Daghero, R.S. Gonnelli, *J. Supercond. Nov. Magn.* **24**, 247, (2011).
- [32] G.A. Ummarino, *Phys. Rev. B* **83**, 092508 (2011).
- [33] L. Boeri, M. Calandra, I.I. Mazin, O.V. Dolgov, F. Mauri, *Phys. Rev. B* **82**, 020506 (2010).
- [34] P.J. Hirschfeld, M.M. Korshunov, and I.I. Mazin, *Rep. Prog. Phys.* **74**, 124508, (2011).
- [35] I.I. Mazin and J. Schmalian, *Physica C* **469**, 614 (2009).
- [36] D.S. Inosov, J.T. Park, P. Bourges, D.L. Sun, Y. Sidis, A. Schneidewind, K. Hradil, D. Haug, C.T. Lin, B. Keimer and V. Hinkov, *Nature Physics* **6**, 178 (2010).
- [37] G. Ghigo, D. Torsello, G.A. Ummarino, L. Gozzelino, M.A. Tanatar, R. Prozorov, and P.C. Canfield, *Phys. Rev. Lett.* **121**, 107001 (2018).
- [38] J. Paglione and R.L. Greene, *Nature Physics* **6**, 645 (2010).
- [39] D.S. Inosov, J.T. Park, A. Charnukha, Yuan Li, A.V. Boris, B. Keimer and V. Hinkov, *Phys. Rev. B* **83**, 214520 (2011).
- [40] G.A. Ummarino, S. Galasso, P. Pecchio, D. Daghero, R. S. Gonnelli, F. Kurth, K. Iida, and B. Holzapfel, *Phys. Status Solidi B* **252**, 821-827 (2015).
- [41] Daniele Torsello, Roberto Gerbaldo, Laura Gozzelino, Makariy A. Tanatar, Ruslan Prozorov, Paul C. Canfield, Gianluca Ghigo, *The European Physical Journal Special Topics* **228**, 719 (2019).
- [42] A.A. Golubov, O.V. Dolgov, A.V. Boris, A. Charnukha, D. L. Sun, C. T. Lin, A.F. Shevchun, A.V. Korobenko, M.R. Trunin, and V.N. Zverev, *JETP Lett.* **94**, 333-337 (2011).
- [43] M. Hemmida, H.-A. Krug von Nidda, A. Gunther, A. Loidl, A. Leithe-Jasper, W. Schnelle, H. Rosner, and J. Sichelschmidt, *Phys. Rev. B* **90**, 205105 (2014).
- [44] V.A. Shestakov, M.M. Korshunov, O.V. Dolgov, *Symmetry* **10** 323 (2018); G.A. Ummarino, *J Supercond Nov Magn* **20** 639 (2007).
- [45] A.A. Golubov, A. Brinkman, O.V. Dolgov, J. Kortus, and O. Jepsen, *Phys. Rev. B* **66**, 054524 (2002).
- [46] D. Torsello, G.A. Ummarino, J. Bekaert, L. Gozzelino, R. Gerbaldo, M.A. Tanatar, P.C. Canfield, R. Prozorov, and G. Ghigo *Phys. Rev. Applied* **13**, 064046 (2020).
- [47] G. Ghigo, G.A. Ummarino, L. Gozzelino, R. Gerbaldo, F. Laviano, D. Torsello, T. Tamegai, *Scientific Reports* **7**, 13029 (2017).